

See discussions, stats, and author profiles for this publication at: <https://www.researchgate.net/publication/305021866>

# Comparison of EEG signal preprocessing methods for SSVEP recognition

Conference Paper · July 2016

DOI: 10.1109/TSP.2016.7760893

CITATIONS

6

READS

429

4 authors:



**Marcin Kołodziej**

Warsaw University of Technology

152 PUBLICATIONS 899 CITATIONS

[SEE PROFILE](#)



**Andrzej Majkowski**

Warsaw University of Technology

115 PUBLICATIONS 495 CITATIONS

[SEE PROFILE](#)



**Lukasz Oskwarek**

Warsaw University of Technology

12 PUBLICATIONS 50 CITATIONS

[SEE PROFILE](#)



**Remigiusz Rak**

Warsaw University of Technology

132 PUBLICATIONS 583 CITATIONS

[SEE PROFILE](#)

Some of the authors of this publication are also working on these related projects:



Detekcja poprawa bezpieczeństwa i warunków pracy", finansowanego w latach 2017-2019 w zakresie badań naukowych i prac rozwojowych przez Ministerstwo Nauki i Szkolnictwa Wyższego/Narodowe Centrum Badań i Rozwoju [View project](#)



Parallel metaheuristics for optimization problems [View project](#)

# Comparison of EEG Signal Preprocessing Methods for SSVEP Recognition

Marcin Kołodziej, Andrzej Majkowski, Łukasz Oskwarek, and Remigiusz J. Rak

Institute of Theory of Electrical Engineering Measurement and Information Systems

Warsaw University of Technology

Warsaw, Poland

remigiusz.rak@ee.pw.edu.pl

**Abstract**—This study was carried out to select EEG signal preprocessing methods to effectively detect and classify Steady State Visually Evoked Potentials (SSVEP). Algorithms, such as: Common Average Reference, Independent Component Analysis (in the task of electrooculography artifacts removing and SSVEP enhancement) and combinations of them were implemented and tested. The best classification accuracy improvement was obtained for CAR and ICA-SSVEP preprocessing methods. Experiments showed high usefulness of these methods in the context of SSVEP detection.

**Keywords**—*spatial filter; steady state visually evoked potentials; SSVEP; electroencephalography; EEG; brain-computer interface; BCI; common average reference; CAR; independent component analysis; ICA*

## I. INTRODUCTION

Sophisticated methods of data preprocessing and analysis are often used in Brain-Computer Interface (BCI) design. A popular BCI standard is based on Steady State Visually Evoked Potentials (SSVEP) [1]. The analysis of visual cortex response to light, flickering with different frequencies, is performed in it [2,3]. As the sources of flickering light LEDs are most commonly used [4,5,6]. This type of interface does not require a long process of user training and enables to achieve relatively high information transfer rate (ITR) [2]. The authors created and tested several preprocessing algorithms of EEG signal that help SSVEP recognition. The methods were tested for stimuli at very close to each other frequencies 5, 6, 7 and 8Hz.

An important problem, hindering the classification, is that the EEG potentials taken from a scalp have poor spatial resolution. Research shows [7] that only about half of the EEG signal energy collected by an electrode comes from the head fragment under it (of radius approximately 3 cm). The rest is coming from further areas of brain, eyes, muscles and various external sources. Fortunately, by using appropriate weights to the potentials taken from different electrodes, we may form completely new signal, containing less undesirable information. In general, creating such a new signal is referred to as spatial filtration [8]. Examples of more advanced methods belonging to this group are: Laplace Filter (LF), Local Average Technique (LAT) or Common Average Reference (CAR). After spatial filtering, the resulting new signal (or signals) comes from a large part or even from all of the electrodes. High popularity has also Blind Source Separation (BSS) [9]. It enables

estimation of source components (including artifacts). Another option is Independent Component Analysis (ICA) [10]. The independence of signals is a stronger assumption than lack of cross-correlation assumed in BSS. The ICA is often used for artifacts elimination. There are many practical algorithms to implement ICA [11].

Preprocessing methods applied to SSVEP based brain-computer interfaces are reviewed in [12]. The most frequently used methods are: bandpass filters, band-stop filters, Common Average Reference and Independent Component Analysis. Therefore, we decided to test and compare these methods. Much attention was paid to the implementation of automated algorithms that do not require cooperation with an expert.

## II. MATERIALS

The EEG data were acquired from 5 users, at the age of 23, 25, 31, 42, and 46. Users were stimulated with flickering green light (LED) of frequencies: 5Hz, 6Hz, 7Hz or 8Hz. The stimulation lasted 30 seconds. A LED of a 1cm diameter was placed at a distance of about 1 meter from user eyes. EEG signals were recorded, with the speed of 256S/s, using 16-channel g.USBamp. The electrodes were placed according to the international 10-20 system (O2, AF3, AF4, P4, P3, F4, Fz, F3, FCz, Pz, C4, C3, CPz, Cz, Oz, O1). The signals were filtered with Butterworth bandpass filter (0.1-100Hz) and notch filter (48-52Hz).

## III. METHODS

Presented below are the methods of preprocessing, used in the course of experiments. Among them there are two prepared by the authors automatic algorithms of efficient ICA use in the processing of the EEG signal (ICA-EOG and ICA-SSVEP).

### A. Raw EEG signal (RAW)

The symbolic RAW name means that any method of EEG signal preprocessing was used. Any frequency or spatial filters were applied.

### B. Common Average Reference (CAR)

Common Average Reference is often used in electroencephalography as well as in BCI. In this case, the electrode potential is calculated by subtracting from its own potential the averaged sum of potentials from all electrodes, according to equation [13]:

$$V_j^{CAR} = V_j^{ER} - \frac{1}{N} \sum_{i=1}^N V_i^{ER} \quad (1)$$

where  $V_j^{ER}$  denotes the potential between the  $j$ -th electrode and a reference electrode and  $N$  is the total number of electrodes used in the experiment. The potential  $V_j^{CAR}$  is determined for all  $N$  electrodes ( $j=1,2,...N$ ).

### C. Independent Component Analysis (ICA)

For ICA calculations, the authors implemented *runica* function from EEGLAB toolbox. It performs decomposition of input data using the ICA algorithm of Bell & Sejnowski [14]. In general, the set of decomposition equations can be presented in matrix form [9]:

$$\mathbf{x} = \mathbf{A}\mathbf{s} + \mathbf{v} \quad (2)$$

where  $\mathbf{x}$  depicts the vector of recorded signals,  $\mathbf{s}$  - a set of independent source signals,  $\mathbf{v}$  - noise vector. In this model source signals are mixed in a linear manner using the weight matrix  $\mathbf{A}$ . In addition, there is a random noise  $\mathbf{v}$ , independent on the source signals. When the mixing matrix  $\mathbf{A}$  is known and the noise  $\mathbf{v}$  is negligible the problem can be solved easily. Otherwise, a separate matrix  $\mathbf{W}$  is sought that satisfies equation:

$$\mathbf{y} = \mathbf{W}\mathbf{x} \quad (3)$$

It would be ideal to obtain the vector  $\mathbf{y}$  equal to the source signals  $\mathbf{s}$ . However, the ICA algorithm enables to determine the  $\mathbf{W}$  matrix in such a way that the  $\mathbf{y}$  components are “most” independent.

In the course of our experiments there were calculated independent components of EEG signals coming from all sessions of all users, what gave an universal separation matrix  $\mathbf{W}$ , common for all stimuli (5, 6, 7 and 8Hz). Such an approach allows a reliable assessment of the effectiveness of the used ICA method.

### D. Automated EOG correction (ICA-EOG)

In the registered EEG signal there may appear artifacts, whose origin is identified with muscle activity (EMG), for example jaw clamping, tongue movement, straining neck muscles, eye movements or blinking (EOG). If we are able to separate them, they can be removed. Independent Component Analysis provides this possibility. The procedure of manual reduction of EOG artifacts by an expert, after ICA application, is well known and widely used [15,16,17]. Also several automatic algorithms are described [18,19,20]. Unfortunately those algorithms are not universal.

We proposed our own method of automatic detection and removal of EOG artifacts. It would be sufficient to remove the ICA component, which has highest correlation with the signal from AF3 electrode (the channel closest to eyes). In the proposed algorithm cross-correlation between each obtained ICA component and the EEG signal collected from the AF3 electrode was calculated. The component with the highest value of cross-correlation was removed from the signal, as the one containing most of EOG artifacts.

### E. Automated SSVEP detection (ICA-SSVEP)

ICA also provides the ability to isolate the components containing the desired EEG potentials, in particular SSVEP. As in the case of artifacts an expert can indicate the proper component through visual evaluation. Our aim was to automate this process. Some methods of automatic detection of SSVEP components are commonly known [21,22].

To automate the SSVEP detection, we assumed that it is sufficient to find the EEG component with the highest cross-correlation with the signal acquired from the Oz channel (greatly influenced by SSVEP) [23]. The EEG signal was divided into short time windows, correlation coefficients were calculated for the corresponding windows and the results were averaged, then the needed component, with the highest correlation was selected. The described steps of signal processing allowed both to improve the signal quality and to find component with a maximum SSVEP content (ICA-SSVEP).

All methods of EEG signal preprocessing together with the description of the obtained signals are presented in Table I. These signals were used in the next stage - the feature extraction process.

TABLE I. EEG PROCESSING STEPS AND THE DESCRIPTION OF OBTAINED SIGNALS

Symbolic name of method	The signal (or component) for further analysis
RAW	Raw signal from Oz electrode
ICA-EOG	Signal from the Oz electrode after the EOG component removal and signal reconstruction
ICA-SSVEP	SSVEP component
RAW-CAR	Signal from the Oz electrode after implementation of CAR spatial filter
ICA-EOG-CAR	Signal from the Oz electrode after the EOG component removal, signal reconstruction and CAR filtration
ICA-SSVEP-CAR	SSVEP component after CAR filtration

### F. Feature extraction

Each obtained signal, described in Table I, was next divided into  $t$ -second time windows, for which feature extraction was done. Experiments were performed for  $t = 1, 2, 4$ s. As features, spectral lines of analyzed signal were used, calculated for frequencies 5, 6, 7, 8Hz and their second and third harmonics (10, 12, 14, 16Hz; 15, 18, 21, 24Hz).

### G. Classification and Testing

As classifiers  $k$  nearest neighbor ( $k$ -NN), linear discriminant analysis (LDA) and quadratic discriminant analysis (QDA) were implemented [24]. For classifier learning and testing 10-fold cross validation test was used [25].

## IV. RESULTS

In Tables II, III, IV there are presented the results of the EEG signal classification for all users (S1-S5), with different signal preprocessing methods, for three harmonics, different time windows and  $k$ -NN classifier ( $k=10$ , 10-CV test). There

are also given averaged classification results for all users (*avgs*) and for all processing methods (*avgm*) and also the corresponding standard deviations.

TABLE II. CLASSIFICATION ACCURACY (K-NN) FOR 1-SECOND WINDOW AND FOR THREE HARMONICS

	S1	S2	S3	S4	S5	avgs	stds
RAW	0,66	0,52	0,36	0,56	0,62	0,54	0,12
ICA-EOG	0,71	0,52	0,31	0,56	0,62	0,54	0,15
RAW-CAR	0,88	0,52	0,33	0,52	0,88	0,62	0,24
ICA-EOG-RAW	0,87	0,56	0,33	0,59	0,86	0,64	0,23
ICA-SSVEP-CAR	0,72	0,71	0,50	0,50	0,74	0,63	0,12
ICA-SSVEP	0,69	0,74	0,56	0,52	0,71	0,64	0,09
avgm	0,75	0,59	0,40	0,54	0,74		
stdm	0,09	0,11	0,10	0,03	0,11		

TABLE III. CLASSIFICATION ACCURACY (K-NN) FOR 2-SECOND WINDOW AND FOR THREE HARMONICS

	S1	S2	S3	S4	S5	avgs	stds
RAW	0,81	0,64	0,52	0,78	0,76	0,70	0,12
ICA-EOG	0,88	0,67	0,51	0,71	0,75	0,70	0,13
RAW-CAR	0,97	0,68	0,52	0,69	0,97	0,77	0,19
ICA-EOG-CAR	0,97	0,73	0,54	0,68	0,99	0,78	0,19
ICA-SSVEP-CAR	0,79	0,94	0,75	0,64	0,87	0,80	0,11
ICA-SSVEP	0,79	0,95	0,71	0,72	0,85	0,80	0,09
avgm	0,87	0,77	0,59	0,70	0,87		
stdm	0,09	0,14	0,11	0,05	0,10		

TABLE IV. CLASSIFICATION ACCURACY (K-NN) FOR 4-SECOND WINDOW AND FOR THREE HARMONICS

	S1	S2	S3	S4	S5	avgs	stds
RAW	0,96	0,79	0,52	0,86	0,82	0,79	0,16
ICA-EOG	0,96	0,79	0,50	0,86	0,82	0,79	0,17
RAW-CAR	0,98	0,80	0,57	0,80	1,00	0,83	0,17
ICA-EOG-CAR	1,00	0,79	0,66	0,79	1,00	0,85	0,14
ICA-SSVEP-CAR	0,89	1,00	0,79	0,59	0,95	0,84	0,16
ICA-SSVEP	0,88	1,00	0,84	0,55	0,93	0,84	0,17
avgm	0,95	0,86	0,65	0,74	0,92		
stdm	0,05	0,11	0,14	0,13	0,08		

TABLE V. CLASSIFICATION ACCURACY (K-NN) FOR 4-SECOND WINDOW AND FOR TWO HARMONICS

	S1	S2	S3	S4	S5	avgs	stds
RAW	0,89	0,77	0,52	0,80	0,84	0,76	0,14
ICA-EOG	0,95	0,82	0,41	0,86	0,84	0,78	0,21
RAW-CAR	0,96	0,73	0,57	0,82	1,00	0,82	0,17
ICA-EOG-CAR	1,00	0,79	0,57	0,80	0,98	0,83	0,17
ICA-SSVEP-CAR	0,88	0,96	0,71	0,61	0,98	0,83	0,16
ICA-SSVEP	0,86	1,00	0,88	0,59	0,95	0,85	0,16
avgm	0,92	0,85	0,61	0,75	0,93		
stdm	0,05	0,10	0,16	0,11	0,07		

TABLE VI. CLASSIFICATION ACCURACY (K-NN) FOR 4-SECOND WINDOW AND FOR 1ST HARMONIC

	S1	S2	S3	S4	S5	avgs	stds
RAW	0,89	0,71	0,41	0,71	0,82	0,71	0,18
ICA-EOG	0,89	0,71	0,48	0,70	0,82	0,72	0,15
RAW-CAR	0,89	0,71	0,46	0,50	0,96	0,71	0,22
ICA-EOG-CAR	0,95	0,75	0,52	0,59	0,95	0,75	0,19
ICA-SSVEP-CAR	0,88	0,91	0,66	0,45	0,73	0,73	0,18
ICA-SSVEP	0,88	0,95	0,82	0,50	0,75	0,78	0,17
avgm	0,90	0,79	0,56	0,57	0,84		
stdm	0,02	0,11	0,15	0,11	0,09		

TABLE VII. CLASSIFICATION ACCURACY (LDA) FOR 4-SECOND WINDOW AND FOR THREE HARMONICS

	S1	S2	S3	S4	S5	avgs	stds
RAW	0,96	0,79	0,61	0,82	0,84	0,80	0,13
ICA-EOG	0,98	0,80	0,59	0,88	0,84	0,82	0,14
RAW-CAR	1,00	0,80	0,54	0,84	1,00	0,84	0,18
ICA-EOG-CAR	1,00	0,80	0,59	0,86	0,98	0,85	0,16
ICA-SSVEP-CAR	0,89	1,00	0,86	0,68	0,96	0,88	0,12
ICA-SSVEP	0,86	1,00	0,89	0,66	0,91	0,86	0,12
avgm	0,95	0,87	0,68	0,79	0,92		
stdm	0,05	0,11	0,15	0,09	0,06		

The classification was also performed for first and second harmonics as features (Table V). Finally the classification was made for only the first harmonic taken as features (Table VI). In turn, Table VII contains the results of classification for LDA classifier using three harmonics.

## V. DISCUSSION

The results of experiments allow us to conclude that relatively computationally simple CAR method enables, in a significant way (by average 4-8%), to improve the classification accuracy, compared to the results obtained for raw signal (RAW). This trend is visible in almost all cases. An example of spectrum of the EEG signal acquired from the Oz electrode (user S1, 7Hz stimuli) is shown in Fig. 1. "CAR" depicts the spectrum of the EEG signal after spatial filtering, "Raw" - raw EEG signal spectrum without the use of preprocessing method, "u" - averaged spectrum calculated for all electrodes.

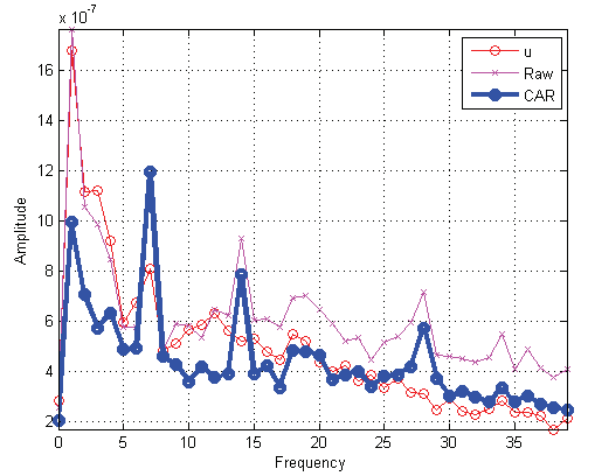


Fig. 1. EEG signal spectrum (Oz electrode) for S1 user and 7Hz stimuli

It can be seen a significant "enhancement" of spectral lines for the frequencies 7, 14, 28Hz what corresponds with 1, 2 and 4 stimulus harmonic. It means that the use of a simple CAR method can enhance the interesting features of EEG signal and can eliminate some artifacts.

To quantify the degree of SSVEP enhancement after CAR implementation  $f_{SNR}$  ratio was defined:

$$f_{SNR} = \frac{2A_f}{A_{f-1} + A_{f+1}} \quad (4)$$

where  $A_f$  is spectral line amplitude for the considered frequency and  $A_{f-1}$ ,  $A_{f+1}$  spectral line amplitudes for frequencies lower and higher by 1Hz. Average values of  $f_{SNR}$  (along all windows) for subsequent harmonics of 5Hz stimulus frequency for S1 user are shown in Table VIII.

TABLE VIII. AVERAGED VALUES OF  $f_{SNR}$  COEFFICIENT FOR USER S1

Method	frequency			
	5Hz	10Hz	15Hz	20Hz
RAW	1,08	1,64	1,00	1,47
RAW-CAR	1,34	2,00	1,04	1,57

It can be seen an increase in the value of  $f_{SNR}$  coefficient for all the considered harmonics caused by using the CAR filter. Amplitude enhancement for the considered frequencies translates easily to the classification accuracy. This is particularly important for the stimuli frequencies close to each other as: 5, 6, 7, 8Hz.

In the experiments, we also examined some methods of automatic removal of EOG artifacts with the use of Independent Component Analysis. An example of the EEG signal after the ICA-EOG correction, using AF3 as an auxiliary electrode, is shown in Fig. 2.

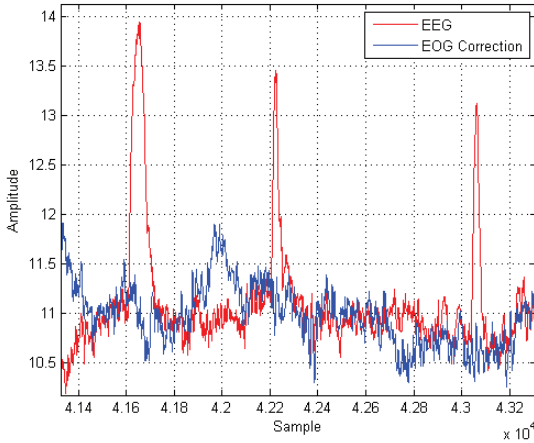


Fig. 2. EEG signal after ICA-EOG preprocessing

The effectiveness of the method is based on the assumption that it is possible to separate an independent EOG component coming from the eyes activity. We focused on finding such an EOG component, which had the greatest correlation with the signal from AF3 electrode. Distribution of weights for the separated ICA-EOG component (high correlation with signals recorded from AF3 electrode) is shown in Fig. 3.

Further research concerned the ICA-EOG-CAR method. In this case, it was observed a slight improvement in the classification accuracy in comparison with the ICA-EOG method. On the other hand, it turned out that using ICA-SSVEP-CAR method gave no improvement or even a slight deterioration of results in comparison with the ICA-SSVEP method.

In summary, the best SSVEP classification results were achieved by prior separation of the ICA component containing the SSVEP. As experiments showed, one could easily separate

SSVEP component for each user. Filtered EEG signal (2-40 Hz Butterworth filter) from Oz electrode of 1s duration, together with a separated ICA-SSVEP component (S2 user, 8 Hz stimulus) is presented in Fig. 4.

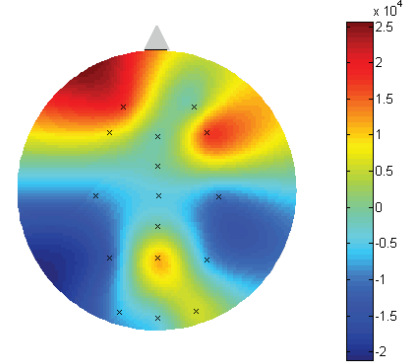


Fig. 3. Distribution of weights for ICA-EOG component

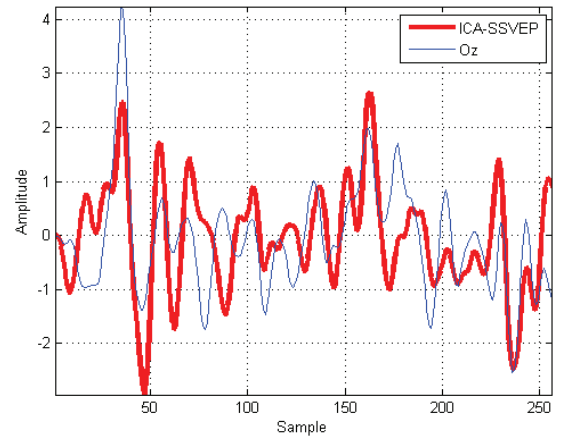


Fig. 4. EEG signal from Oz electrode and separated ICA-SSVEP component (S1 user, 8Hz stimuli)

In Fig. 5 there are shown the spectra of filtered (Butterworth 2-40Hz) one second signal segments together with ICA-SSVEP component (S2 user, 8 Hz stimulus). It can be noticed that the ICA-SSVEP component is "enhanced" for 8Hz (1 harmonic).

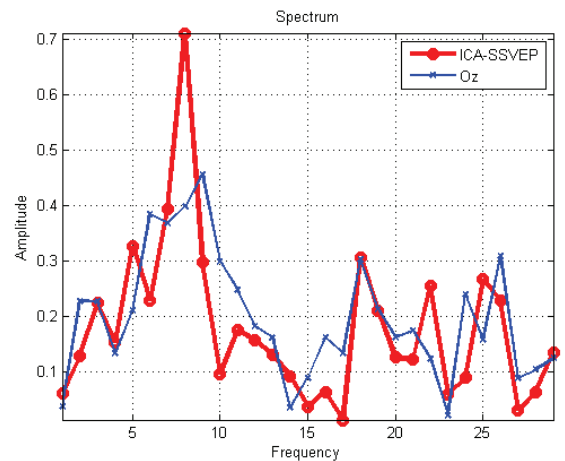


Fig. 5. The EEG signal spectrum for Oz electrode and ICA-SSVEP component



Distribution of weights for separated ICA-SSVEP component (high correlation with signals recorded from Oz electrode) is illustrated in Fig. 6. The largest values of weights match the visual cortex location.

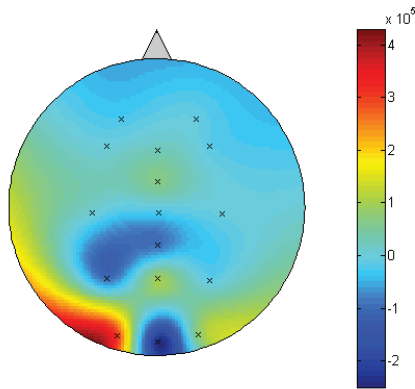


Fig. 6. Distribution of weights for ICA-SSVEP component

Compared to classification of RAW signals from Oz electrode, using ICA-SSVEP we achieved an increase in the classification accuracy of about 8%. However, there were isolated cases, where the proposed method worsened classification results.

The comparison of average classification accuracies for all examined methods is presented in Fig. 7. The effectiveness of preprocessing methods, mostly depends on the quality of the raw signal. It is largely individual (personal) feature.

But also the width of used time window, for which features were calculated is very important. The best results were obtained for 4s window width, for three harmonics and LDA classifier. The average classification accuracy using RAW method (without preprocessing) was 0.8, using RAW-CAR method - 0.84, and ICA-SSVEP - 0.86. Such classification accuracy would allow to obtain ITR between 25 and 30 bits/min.

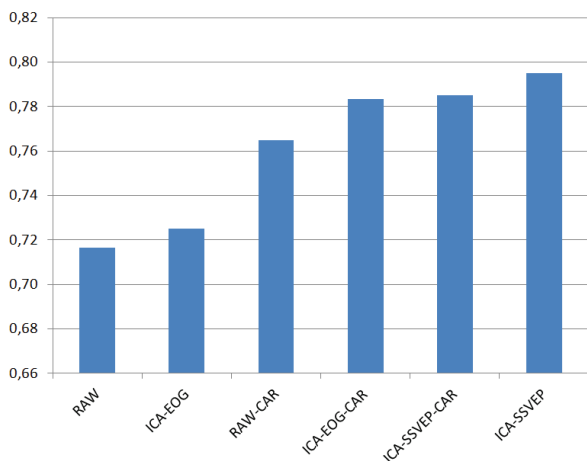


Fig. 7. The average SSVEP classification accuracy for the various preprocessing methods of the EEG signal

In experiments conducted by the authors, best results were obtained for S1 and S5 users, thanks to relatively good quality of "generated" SSVEP. Interestingly, the greatest increases in classification accuracy, achieved thanks to the preprocessing methods, were observed for S2 and S3 users, for whom SSVEP were relatively poor. So for people with weak SSVEP signals, using sophisticated data preprocessing methods makes sense. In order to confirm this thesis, the results of our analyzes were confronted with the current densities obtained using the LORETA software [26]. The results achieved using LORETA for users S1 (good) and S3 (bad) are shown in Fig. 8.

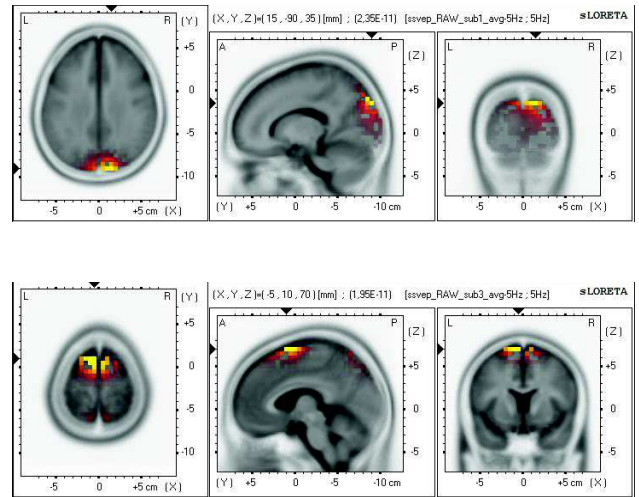


Fig. 8. The results illustrating the current densities obtained using LORETA software for S1 (top) and S3 (bottom) users

It turned out that in case of persons for whom classification accuracy of RAW signals were poor, LORETA also showed weak power of generated SSVEP. For example, for S1 user the maximum current density for stimuli frequency 5Hz was  $23,5\mu\text{A}/\text{mm}^2$ , and for S3 user only  $19,5\mu\text{A}/\text{mm}^2$ . LORETA analysis results showed that for S3 user, in contrast to S1 user, SSVEP for 5Hz dominated not in the visual cortex but in the frontal brain region.

## VI. CONCLUSION

In the article the authors presented consistent comparison of the most popular methods of EEG signal preprocessing to facilitate subsequent SSVEP classification process. Automatic algorithms such as: Common Average Reference, Independent Component Analysis (in the task of EOG artifact removing and SSVEP enhancement) and combinations of these algorithms were implemented and tested. Experiments show that the best results (classification accuracy improvement) was obtained for CAR and ICA-SSVEP preprocessing for off-line methods. The developed preprocessing algorithms that use ICA are more difficult to implement on-line. While the CAR algorithm can be used without any problem in any BCI based on SSVEP. In addition, it was observed that the sophisticated preprocessing methods improved classification results particularly in users with low SSVEP.

## REFERENCES

- [1] R. J. Rak, M. Kołodziej, and A. Majkowski, "Brain-computer interface as measurement and control system the review paper," *Metrol. Meas. Syst.*, vol. 19, no. 3, pp. 427–444, 2012.
- [2] M. K. Reagor, C. Zong, and R. Jafari, "Maximizing information transfer rates in an SSVEP-based BCI using individualized Bayesian probability measures," *Conf. Proc. Annu. Int. Conf. IEEE Eng. Med. Biol. Soc. IEEE Eng. Med. Biol. Soc. Annu. Conf.*, vol. 2014, pp. 654–657, 2014.
- [3] S. Mouli, R. Palaniappan, I. P. Sillitoe, and J. Q. Gan, "Performance analysis of multi-frequency SSVEP-BCI using clear and frosted colour LED stimuli," in *2013 IEEE 13th International Conference on Bioinformatics and Bioengineering (BIBE)*, 2013, pp. 1–4.
- [4] P. J. Durka, R. Kuś, J. Żygierewicz, M. Michalska, P. Milanowski, M. Łabęcki, T. Spustek, D. Laszuk, A. Duszyk, and M. Kruszyński, "User-centered design of brain-computer interfaces: OpenBCI.pl and BCI Appliance," *Bull. Pol. Acad. Sci. Tech. Sci.*, vol. 60, no. 3, 2012, pp. 427–431.
- [5] M. Byczuk, P. Poryżala, and A. Materka, "On diversity within operators' EEG responses to LED-produced alternate stimulus in SSVEP BCI," *Bull. Pol. Acad. Sci. Tech. Sci.*, vol. Vol. 60, no. nr 3, 2012, pp. 447–453.
- [6] D. Zhu, J. Bieger, G. Garcia Molina, R. M. Aarts, D. Zhu, J. Bieger, G. Garcia Molina, and R. M. Aarts, "A Survey of Stimulation Methods Used in SSVEP-Based BCIs, A Survey of Stimulation Methods Used in SSVEP-Based BCIs," *Comput. Intell. Neurosci. Comput. Intell. Neurosci.*, vol. 2010, 2010, p. e702357, Mar. 2010.
- [7] P. L. Nunez, R. Srinivasan, A. F. Westdorp, R. S. Wijesinghe, D. M. Tucker, R. B. Silberstein, and P. J. Cadusch, "EEG coherency: I: statistics, reference electrode, volume conduction, Laplacians, cortical imaging, and interpretation at multiple scales," *Electroencephalogr. Clin. Neurophysiol.*, vol. 103, no. 5, Nov. 1997, pp. 499–515.
- [8] H. Klekowicz, U. Malinowska, A. J. Piotrowska, D. Wołyńczyk-Gmaj, S. Niemcewicz, and P. J. Durka, "On the robust parametric detection of EEG artifacts in polysomnographic recordings," *Neuroinformatics*, vol. 7, no. 2, Jun. 2009, pp. 147–160.
- [9] A. Cichocki and S. Amari, *Adaptive Blind Signal and Image Processing: Learning Algorithms and Applications*. New York, NY, USA: John Wiley & Sons, Inc., 2002.
- [10] A. Hyvärinen and E. Oja, "A Fast Fixed-Point Algorithm for Independent Component Analysis," *Neural Comput.*, vol. 9, no. 7, Oct. 1997, pp. 1483–1492.
- [11] A. Hyvärinen, J. Karhunen, and E. Oja, *Independent Component Analysis*. John Wiley & Sons, 2004.
- [12] Q. Liu, K. Chen, Q. Ai, and S. Q. Xie, "Review: recent development of signal processing algorithms for SSVEP-based brain computer interfaces," *J Med Biol Eng*, 2013.
- [13] D. J. McFarland, L. M. McCane, S. V. David, and J. R. Wolpaw, "Spatial filter selection for EEG-based communication," *Electroencephalogr. Clin. Neurophysiol.*, vol. 103, no. 3, Sep. 1997, pp. 386–394.
- [14] A. J. Bell and T. J. Sejnowski, "An Information-Maximization Approach to Blind Separation and Blind Deconvolution," *Neural Comput.*, vol. 7, no. 6, Nov. 1995, pp. 1129–1159.
- [15] T.-P. Jung, S. Makeig, M. Westerfield, J. Townsend, E. Courchesne, and T. J. Sejnowski, "Removal of eye activity artifacts from visual event-related potentials in normal and clinical subjects," *Clin. Neurophysiol.*, vol. 111, no. 10, Oct. 2000, pp. 1745–1758.
- [16] R. N. Vigário, "Extraction of ocular artefacts from EEG using independent component analysis," *Electroencephalogr. Clin. Neurophysiol.*, vol. 103, no. 3, Sep. 1997, pp. 395–404.
- [17] T.P. Jung, S. Makeig, C. Humphries, T.-W. Lee, M. J. McKEOWN, V. Iragui, and T. J. Sejnowski, "Removing electroencephalographic artifacts by blind source separation," *Psychophysiology*, vol. 37, no. 02, Mar. 2000, pp. 163–178.
- [18] A. Schlögl, C. Keinrath, D. Zimmermann, R. Scherer, R. Leeb, and G. Pfurtscheller, "A fully automated correction method of EOG artifacts in EEG recordings," *Clin. Neurophysiol.*, vol. 118, no. 1, Jan. 2007, pp. 98–104.
- [19] G. L. Wallstrom, R. E. Kass, A. Miller, J. F. Cohn, and N. A. Fox, "Automatic correction of ocular artifacts in the EEG: a comparison of regression-based and component-based methods," *Int. J. Psychophysiol.*, vol. 53, no. 2, Jul. 2004, pp. 105–119.
- [20] C. A. Joyce, I. F. Gorodnitsky, and M. Kutas, "Automatic removal of eye movement and blink artifacts from EEG data using blind component separation," *Psychophysiology*, vol. 41, no. 2, Mar. 2004, pp. 313–325.
- [21] Y. Wang, Z. Zhang, X. Gao, and S. Gao, "Lead selection for SSVEP-based brain-computer interface," in *26th Annual International Conference of the IEEE Engineering in Medicine and Biology Society, 2004. IEMBS '04*, 2004, vol. 2, pp. 4507–4510.
- [22] S. Pouryazdian and A. Erfanian, "Detection of Steady-State Visual Evoked Potentials for Brain-Computer Interfaces Using PCA and High-Order Statistics," in *World Congress on Medical Physics and Biomedical Engineering, September 7 - 12, 2009, Munich, Germany*, O. Dössel and W. C. Schlegel, Eds. Springer Berlin Heidelberg, 2009, pp. 480–483.
- [23] B. Allison, T. Luth, D. Valbuena, A. Teymourian, I. Volosyak, and A. Graser, "BCI Demographics: How Many (and What Kinds of) People Can Use an SSVEP BCI?," *IEEE Trans. Neural Syst. Rehabil. Eng.*, vol. 18, no. 2, Apr. 2010, pp. 107–116.
- [24] A. Schlögl, F. Lee, H. Bischof, and G. Pfurtscheller, "Characterization of four-class motor imagery EEG data for the BCI-competition 2005," *J. Neural Eng.*, vol. 2, no. 4, p. L14, 2005.
- [25] O. Dehzangi, V. Nathan, C. Zong, C. Lee, I. Kim, and R. Jafari, "A novel stimulation for multi-class SSVEP-based brain-computer interface using patterns of time-varying frequencies," in *2014 36th Annual International Conference of the IEEE Engineering in Medicine and Biology Society (EMBC)*, 2014, pp. 118–121.
- [26] R. D. Pascual-Marqui, M. Esslen, K. Kochi, and D. Lehmann, "Functional imaging with low-resolution brain electromagnetic tomography (LORETA): a review," *Methods Find. Exp. Clin. Pharmacol.*, vol. 24 Suppl C, pp. 91–95, 2002.